



Research Article

# The influence of anhydrite III as cement replacement material in production of lightweight masonry blocks for unreinforced non-load bearing walls

Şevket Onur KALKAN<sup>id</sup>, Lütfullah GÜNDÜZ<sup>id</sup>

Department of Civil Engineering, İzmir Katip Çelebi University, İzmir, Türkiye

## ARTICLE INFO

### Article history

Received: 24 October 2022

Revised: 04 December 2022

Accepted: 08 December 2022

### Key words:

Anhydrite III, calcium sulfate, cement replacement, compressive strength of masonry, lightweight concrete, masonry block, thermal conductivity

## ABSTRACT

Lightweight cellular hollow concrete (LCHC) block is a masonry unit with excellent thermal and acoustic performance, fire resistance, and high weathering resistance manufactured by precast technique. This work presents an experimental study that investigates the effects of partial volumetric replacement of Portland cement by calcium sulfate anhydrite on precast properties, especially the hardening time of the products, thermal insulation properties, and mechanical properties of the LCHCs. LCHC block is produced by the mixing of Portland cement (PC), anhydrite III (ANH), expanded perlite (EP), pumice (PU), and calcite (CA) for building applications. Experimental studies were carried out on both 10x10x10 cm<sup>3</sup> cube specimens and 19x19x39 cm<sup>3</sup> block specimens with 16 different mixture batches. The unit weights and compressive strengths of the cube specimens decreased as the ANH replacement level increased, depending on the decrease in the cement ratio. However, it was observed that the compressive strength of the block specimens increased up to the volumetric replacement level of 1.86%. As expected, the specimens' thermal conductivity values decreased with the unit weight. The most notable change in the specimens occurred during the hardening time. The hardening process of the specimens can be completed up to 90 times faster than the control mixture. In addition, within the scope of the study, three formulations are presented in which the compressive strength and the elastic modulus of the wall sections made with LCHC blocks can be calculated, and the thermal conductivity value of the masonry block unit can be calculated.

**Cite this article as:** Kalkana, ŞO., & Gündüz, L. (2022). The influence of anhydrite III as cement replacement material in production of lightweight masonry blocks for unreinforced non-load bearing walls. *J Sustain Const Mater Technol*, 7(4), 322–338.

## 1. INTRODUCTION

Lightweight concrete masonry units are mainly used to construct walls as a building material. To produce normal-weight concrete masonry units, a fresh concrete mixture is commonly used: Portland cement, water, sand, and

gravel. This practice produces a light grey colored concrete block with a fine surface texture and a sufficiently high compressive strength. Load-bearing walls and partitions are generally built with these types of blocks. The mass of these types of concrete blocks generally ranges from 16 kg to 27 kg [1]. While the amount of sand in the concrete mixture

\*Corresponding author.

\*E-mail address: [onur\\_kalkan@hotmail.com](mailto:onur_kalkan@hotmail.com)



prepared for concrete blocks is higher than the typical concrete mixture, the amount of gravel and water is less. The resulting concrete block is commonly called a lightweight masonry block when lightweight aggregates are used instead of normal-weight sand and gravel in the fresh mixture. This process achieves more porous and lighter concrete blocks with a medium-to-coarse surface texture, good strength, good sound-deadening properties, and a higher thermal insulating value than a normal-weight concrete block. LCHC blocks can be produced by mixing lightweight aggregates, cement, and water to construct non-load-bearing infill walls and slabs. Lightweight concrete blocks can be manufactured with densities ranging from 400 kg/m<sup>3</sup> to 1100 kg/m<sup>3</sup>, affecting an average reduction in dead load of 40% to 50% compared to buildings with conventional concrete walls [2–4]. The mass of a typical lightweight concrete block is usually between 5 and 14 kg, depending on the aggregate type, shape, and grading [1].

Lightweight aggregates generally have maximum dry loose bulk densities of about 880 kg/m<sup>3</sup> for the coarse fractions and 1040 kg/m<sup>3</sup> for all-in aggregates [5]. Depending on their final source, lightweight aggregates are also classified as natural and artificial. The primary natural lightweight aggregates are diatomite, pumice, scoria, volcanic slug, and volcanic tuff. Except for diatomite, all are volcanic in origin. Pumice and scoria are more widely used for hollow and solid concrete block production in Türkiye [6, 7]. Also, using the expanded perlite in lightweight concrete productions and hollow block cavities is involved in studies mostly for thermal insulation [8–11]. On the other hand, most of the studies only investigate the use of cement as a binding material. There are not enough studies on cement and gypsum as dual-binder systems.

Gypsum is one of the most common mineral binders for building materials. The use of chemical additives, the use of mineral additives, the addition of cement, the addition of lime, and the use of reinforcement materials allow for obtaining various properties for gypsum binders [12]. The main component of this material is calcium sulfate, which can be found in hydrous and non-hydrous compounds: dihydrate (CaSO<sub>4</sub>·2H<sub>2</sub>O), hemihydrate (CaSO<sub>4</sub>·0.5H<sub>2</sub>O), and anhydrite (CaSO<sub>4</sub>). Gypsum has many advantages thanks to its unique performance. These advantages can generally be evaluated as recyclability, non-toxicity, high sound and heat insulation ability, easy application, and rapid hardening. However, its most important feature is that it is the material with the least CO<sub>2</sub> emission during its production, among the most used binding materials in building materials, which are gypsum, lime, and cement. Hemihydrate production from mineral gypsum requires about 150 °C heating and about 350 °C heating for anhydrite, while that of Portland cement requires about 1450 °C calcination heat and lime requires 900 °C calcination heat. Compared to lime and cement, the total CO<sub>2</sub> emission of gypsum is relatively low.

Gypsum binders are produced by heating the gypsum mineral (CaSO<sub>4</sub>·2H<sub>2</sub>O) at specific temperatures. As the temperature increases, the gypsum mineral begins to dehydrate, and gypsum with lower H<sub>2</sub>O content begins to be produced. Calcium sulfate hemihydrate (CaSO<sub>4</sub>·0.5H<sub>2</sub>O) is formed when 1.5 mol of H<sub>2</sub>O is lost. The hemihydrate is formed under ambient conditions from 45 °C to 200 °C temperature range [13]. Further heating of calcium sulfate hemihydrate leads to soluble anhydrite (anhydrite III, CaSO<sub>4</sub>) [14]. By heating the gypsum mineral at a sufficient temperature, two types of hemihydrate or anhydrite binders can be produced depending on the equipment applied and technological parameters: α- and β-hemihydrate or anhydrite. Compared to the α-modification, the specific surface area of the β-modification is larger and more porous. Therefore, the β-modification has a higher water requirement and lower strength [15, 16]. After the formation of anhydrite III, continued heating leads to less soluble anhydrite (anhydrite II). Under ambient conditions, CaSO<sub>4</sub>·II reacts very slowly with water; hence, the name dead burnt gypsum is also given to this mineral [17]. Anhydrite I is formed at temperatures above 1180 °C [14].

Due to the high CO<sub>2</sub> emission values originating from cement production, reducing the cement ratio by cement replacement in cement-binding building materials is among the research topics that have been given importance in recent years from ecological points of view [18, 19]. Therefore, using other binders or cement replacement materials has been the subject of many publications [20]. Cement-based materials should offer economic and environmental benefits besides physical and mechanical properties. For this reason, many studies have been made in the literature to reduce the cement amount of concrete derivative materials by cement replacement method [20–22].

Gypsum is widely used in cement production as a calcium sulfate activator. However, the usage level is currently limited to about 5% of cementitious material because of its high sulfate content. It is mainly considered that large amounts of sulfate in cement-based materials would cause excessive expansion and cracking [23, 24]. Therefore, the number of studies with gypsum replacement for cement in cement-based building materials is very few. Researchers supported cement-gypsum combination with pozzolans to eliminate the harmful effect of ettringite minerals formed in the microstructure due to using cement and gypsum-derived materials and obtained positive results [25–27].

Concrete masonry units are manufactured with very dry, stiff concrete mixtures. The "no-slump" or "low-slump" material is placed into molds, vibrated, compacted, and demolded quickly. The demolded units are stiff enough to hold their shape as they enter the curing chamber. Afterward, they are palletized and readied for shipping [11]. However, since the products are immediately removed from the mold due to the production method, LCHC blocks that have not gained enough strength may suffer wastage due to breakage.

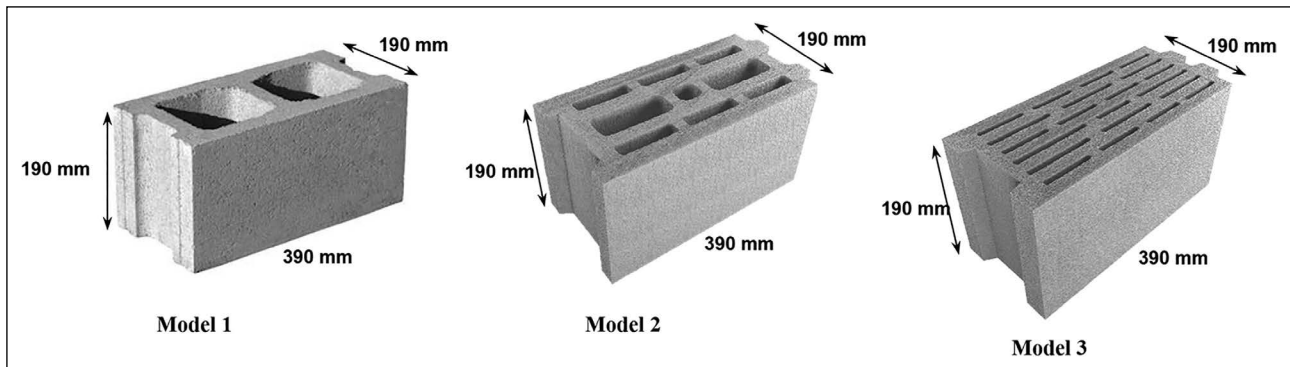


**Figure 1.** The three different models of masonry units.

For this reason, in this study, cement binder and anhydrite gypsum binder were used together with the replacement method in order to gain rapid strength to the products and to bring the products out of production into use quickly. In addition, it is thought that with less cement, the impact on the environment resulting from cement production will decrease, and sustainable building materials can be produced. The present experimental work evaluated the cementitious matrix modified by partial volumetric replacement of the ordinary Portland cement by anhydrite III to produce LCHC blocks as a building material. The effects of anhydrite III on precast properties, the incredibly initial hardening time of the products, thermal insulation properties, mechanical properties, and water absorption of the blocks were investigated. In light of previous literature studies, micronized pumice with high pozzolanic activity was also used in the design of the mixture in order to eliminate the adverse effects of ettringite formation. Pumice and expanded perlite were used as lightweight aggregates for the blocks to be included in the lightweight block category. Also, within the scope of the study, three formulations are presented in which the compressive strength and modulus of elasticity of the walls made with LCHC blocks and the thermal conductivity value of the masonry block unit can be calculated.

## 2. EXPERIMENTAL STUDY

### 2.1. Materials Used in the Research

In this study, three block designs with different cavity geometry are used, provided their outer dimensions are the same. The lightweight concrete masonry hollow blocks with dimensions of 185 mm height, 390 mm length, and 190 mm width, which are generally used for Türkiye, were used throughout the experimental work. The three models of masonry units are shown in Figure 1. Some physical properties of the three models are given in Table 1.

CEM I 42.5N Portland cement was used as a binder.

The  $\beta$ -modification anhydrite III binder was used as a partial replacement material for cement in the test batches. Anhydrite was obtained from a production facility in Türkiye.

**Table 1.** Geometrical properties of the block models

Model number	Cellular holes	$\psi(\text{cm}^2)$	$\eta(\text{dm}^3)$
1	2	321	7.97
2	9	462	10.11
3	21	567	10.78

$\psi$ : Filled surface area of masonry units;  $\eta$ : Net fullness ratio of masonry units by volume.

Two different aggregates, relatively light in terms of density, were used to produce lightweight concrete mix and lightweight blocks. These are expanded perlite (EP) and pumice (PU). The grain size of the expanded perlite was 0/3 mm, and the grain size of the pumice was 0/4 mm. In addition, calcite (CA) with 0/1 mm grain size distribution was used as filling material in the mixture designs.

As mentioned earlier, although the inclusion of extra sulfate in the cement matrix is seen as a disadvantage, with the experience gained from the literature studies, micronized pumice material with a strong pozzolanic effect was used to eliminate the effect of this disadvantage. Natural pozzolans constitute a part of the lightweight aggregate group that could increase the strength and durability of concrete in the production of block-making mixtures. Pumice aggregate in powder form is one of the well-known pozzolans used in concrete applications. 4% by weight of the pumice aggregate used in this study, which has a particle size distribution of 0/4 mm, consists of micronized pumices with a smaller size than 45  $\mu\text{m}$  and high pozzolanic activity. The pozzolanic material minimizes the deleterious effect of the extra sulfate in the cement matrix.

The chemical composition of the cement, anhydrite, EP, PU, and CA used in this research are given in Table 2.

Specific gravity, dry bulk density, and water absorption values of EP, PU, and CA are given in Table 3 and were determined according to the BS 812:P2 [28], BS 812:P110 [29], ASTM C127 [30] and ASTM C128 [31].

**Table 2.** Chemical compositions of CEM I, ANH, EP, PU, and CA (mass %)

Major element	CEM I	ANH	EP	PU	CA
SiO <sub>2</sub>	20.92	2.35	74.14	74.16	0.15
Al <sub>2</sub> O <sub>3</sub>	5.18	0.74	12.35	13.47	0.14
Fe <sub>2</sub> O <sub>3</sub>	3.87	0.31	0.79	1.46	0.10
CaO	62.44	43.35	1.87	1.22	55.09
Na <sub>2</sub> O	0.19	–	3.45	2.76	–
K <sub>2</sub> O	0.78	0.11	4.66	3.13	–
MgO	2.45	2.64	0.48	0.41	1.12
SO <sub>3</sub>	2.48	45.45	–	–	–
LOI	1.51		1.16	3.08	42.86

**Table 3.** Physical properties of EP, PU, and CA

Material	Particle size (mm)	Specific gravity	Dry bulk density (kg/m <sup>3</sup> )	Water absorption (wt %)
P	0/1	2.30	105	41.4
PU	0/4	2.32	780	28.9
CA	0.1/0.8	2.70	1400	1.80

**2.2. Mix Design and Specimen Preparation**

In order to analyze the use of ANH to produce LCHC blocks for walls and partitions, 16 different mixture proportions (B0–B15) adopted for the concrete mixture batches. The mix proportion of test specimens are presented in Table 4.

B0 coded mixture was considered a control mixture, and anhydrite III binding material was not used in this mixture. In the specimens named from B1 to B15, anhydrite III binder has been replaced by volume instead of cement. Also, Table 4 shows weight replacement ratios corresponding to volume replacement ratios are given. The ratios of EP, PU, and CA entering the fresh mixture were kept constant in all batches. The concrete design methodology was constructed according to TS EN 771-3 standard [32].

In the first stage of this experimental study, 10x10x10 cm<sup>3</sup> cube specimens were produced (Fig. 2) using the mixture design given in Table 4. Compressive strength, unit weight, water absorption, and initial hardening time tests were carried out on cube specimens. For each batch of mixtures, three specimens were produced to be used in compressive strength and unit weight tests, three were produced in initial hardening time tests, and three were produced to be used in water absorption tests; in total, nine specimens for each batch. A total of 144 cube specimens were produced for 16 different mixtures.

In this study, the value defined as the *initial hardening time* was evaluated as the time required for the cube specimens to reach a strength value of 1 MPa from when they were removed from the mold. The value of 1 MPa has been experienced as the appropriate strength value predicted in

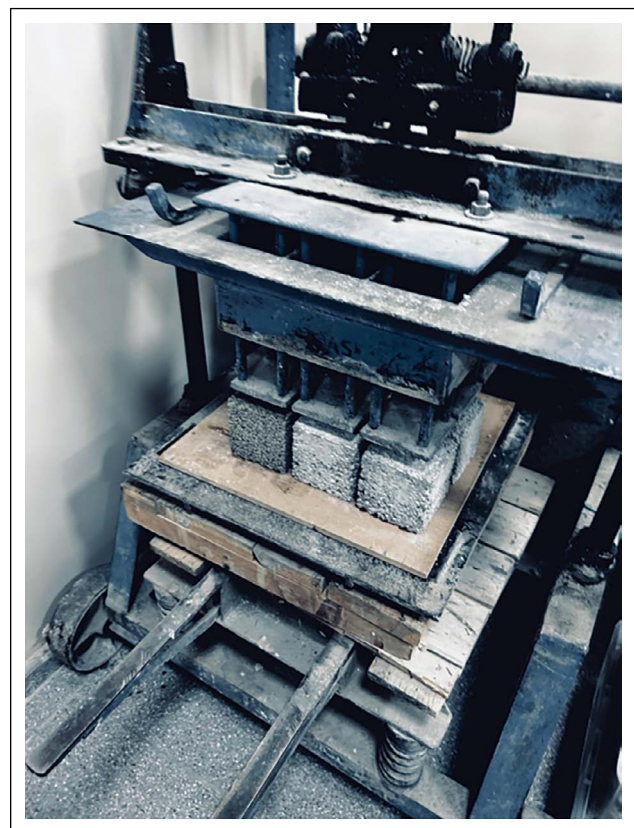


**Figure 2.** Cubic specimen production process.

real applications regarding the transport of the specimens to the area to be applied, the required strength, and permanence during the application. For this reason, it has been accepted, based on the author's experience, that the blocks produced from specimens reaching a compressive strength of 1 MPa are suitable for real applications.

In the second stage of the experimental study, using the mixture design in Table 4, the 16 different mix designs were adapted to each of the three-block models. The second stage was carried out on 19x19x39 cm<sup>3</sup> block specimens. Block geometry for each model is given in Table 1. Unit weight,

**Table 4.** Proportions of trial mixtures (% by volume)

Mix	Binder		ANH (wt% in total binder)	EP	PU	CA
	CEM I	ANH				
0	0.00	10.35	0.00	35.00	45.00	9.65
1	0.31	10.04	3.00	35.00	45.00	9.65
2	0.83	9.52	8.00	35.00	45.00	9.65
3	1.24	9.11	12.00	35.00	45.00	9.65
4	1.86	8.49	18.00	35.00	45.00	9.65
5	2.59	7.76	25.00	35.00	45.00	9.65
6	3.42	6.93	33.00	35.00	45.00	9.65
7	3.93	6.42	38.00	35.00	45.00	9.65
8	4.35	6.00	42.00	35.00	45.00	9.65
9	4.66	5.69	45.00	35.00	45.00	9.65
10	4.97	5.38	48.00	35.00	45.00	9.65
11	5.38	4.97	52.00	35.00	45.00	9.65
12	5.69	4.66	55.00	35.00	45.00	9.65
13	6.00	4.35	58.00	35.00	45.00	9.65
14	6.73	3.62	65.00	35.00	45.00	9.65
15	7.76	2.59	75.00	35.00	45.00	9.65

compressive strength, water absorption, and thermal conductivity tests were carried out on LCHC block specimens. In addition, a formula has been proposed in which the thermal conductivity of the blocks can be calculated based on the compressive strength and the block net fullness ratio without performing a thermal conductivity test. BS 1881: Part 125 [33] was followed for mixing and sampling the fresh concrete in the laboratory, and BS 1881: Part 114 [34] was followed for measuring the density of hardened concrete. A cellular hollow block form confirming the specifications of BS 6073: Part 1 [35] standard was used for the preparation of LCHC specimens.

For each mixture and each block model, nine specimens were produced, a total of 27 blocks for one mixture design. 144 LCHC blocks were produced and tested for 16 different mix designs. The specimens were then air cured at  $22 \pm 3^\circ\text{C}$  and  $50 \pm 5\%$  relative humidity for up to 28 days until testing. The specimens were tested in air-dry conditions for compressive strength by BS 6073: Part 1 [35]. A measurement setup was used for the thermal conductivity test in which the hot box device methodology developed under laboratory conditions was applied. In the Hot Box method, thermal conductivity measurement can be made for the test sample, optionally for temperature environments ranging from  $0^\circ\text{C}$  to  $+55^\circ\text{C}$ . The temperature value on each sample surface was measured from at least 9 points to form a grid on the surface. The thermal conductivity device consists of an electrical heater called the hot room, the section where the sample is placed, and the cold room. The temperature

sensors in both the cold and hot chambers were fully contacted with the sample surface without damage, and the sample surface temperature values were measured with an accuracy of  $0.1^\circ\text{C}$ . The given heat can be controlled with a continuously variable (20–400 watt) current. Since the heat transfer is three-dimensional, the test device is designed to minimize errors. Before recording the temperature data, the sample was stabilized, and data recording was started after reaching the steady state. The desired temperature difference on both surfaces of the test sample placed in the apparatus was provided by the electrical power ( $Q_T$ , Watt) applied to the heater, and the temperature difference between the surfaces was determined as the average value ( $\Delta T$ ,  $^\circ\text{C}$ ) from the measurement values. The thermal conductivity value ( $\lambda$ ,  $\text{W/mK}$ ) of the test sample was calculated using the following equation:

$$\lambda = \frac{Q_T \times d}{A \times \Delta T} \quad (1)$$

Here;

$\lambda$ , thermal conductivity value of the test sample, ( $\text{W/mK}$ ),

$Q_T$ , electrical power applied to the heater (Watts),

$D$ , sample thickness, (m),

$A$  heated area in the heating section ( $\text{m}^2$ ),

$\Delta T$  = temperature difference between surfaces, ( $^\circ\text{C}$ ),

In the last stage of the study, the compressive strength value and elasticity modulus value of the non-load bearing wall, which is built with these block elements and unreinforced, using 0.7 mm thick masonry mortar only in a

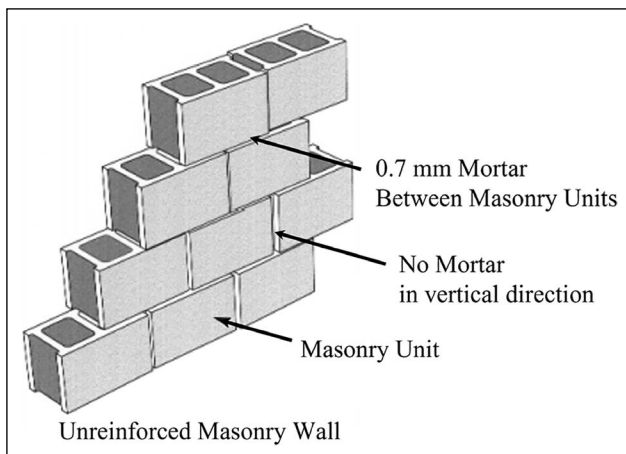


Figure 3. Wall section model.

horizontal position, has been examined. The wall section is presented in Figure 3. By comparing the obtained wall strength values with the technical values predicted in Eurocode 6, the effects of the use of anhydrite in the production of masonry blocks on the mechanical performance of the wall section were tried to be analyzed.

### 3. RESULTS AND DISCUSSIONS

#### 3.1. Cube Specimens

In the first stage of the study, cube specimens were produced, and these specimens' physical and mechanical properties were determined. The physical and mechanical properties of the cube specimens are summarized in Table 5.

Table 5. Physical characteristics of the 100 mm-cube specimens

Mix	Dry density (kg/m <sup>3</sup> )	Compressive strength (N/mm <sup>2</sup> )	Water absorption (% by weight)	A/B
C0	762	2.97	21.1	3.73
C3	758	2.91	21.3	3.75
C8	757	2.89	21.7	3.77
C12	756	2.81	21.8	3.80
C18	756	2.79	22.2	3.83
C25	754	2.71	22.4	3.87
C33	751	2.60	22.7	3.92
C38	750	2.48	23.3	3.95
C42	749	2.46	23.4	3.98
C45	747	2.41	23.8	4.00
C48	745	2.36	24.1	4.01
C52	744	2.34	24.2	4.04
C55	740	2.26	24.4	4.06
C58	738	2.15	24.7	4.08
C65	737	2.12	24.9	4.13
C75	732	1.88	25.4	4.20

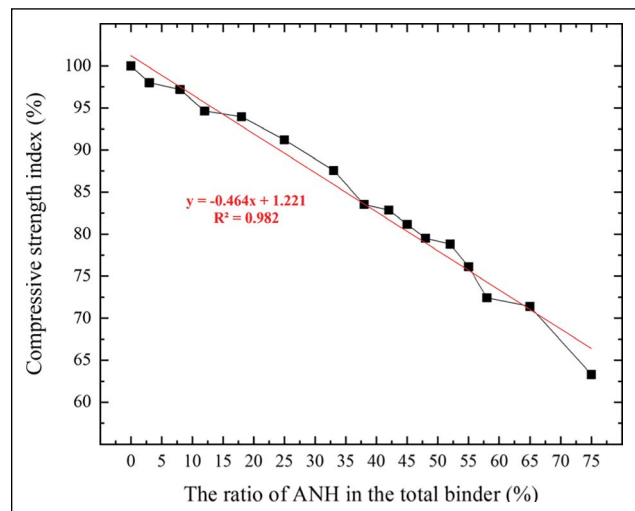
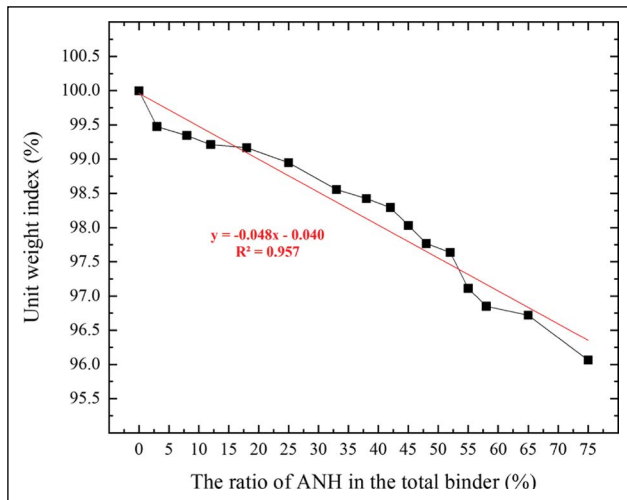


Figure 4. Compressive strength indices of cube specimens versus ANH as a percentage of binder.

The mixtures were coded according to the ANH replacement level, where "C" defines the cubic specimens, and the numbers 0 to 75 define the replacement level of ANH by cement by weight. The water/total binder ratio was kept constant in all mixtures, and the W/B ratio was used as 0.21.

#### 3.1.1 Compressive Strength

Figure 4 shows the compressive strength results for the fifteen trial mixtures at 28 days of curing. The compressive strength of the control batch was 2.97 MPa (i.e., 100%). The compressive strength indices of cube specimens were linearly decreased with increasing ANH replacement levels.



**Figure 5.** Unit weight indices of cube specimens versus ANH as a percentage of binder.

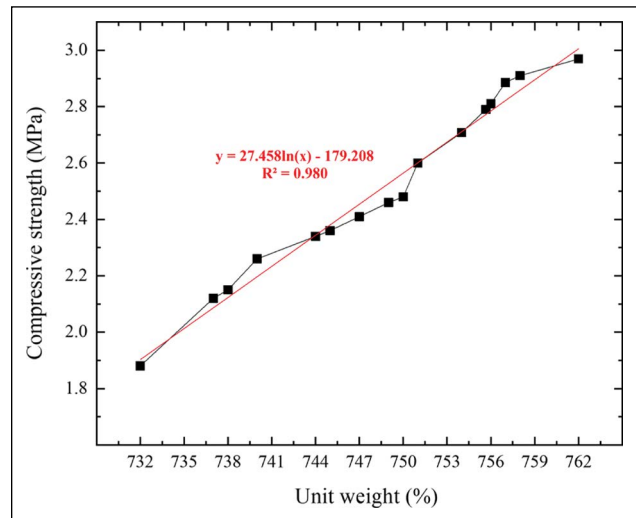
In cube specimens, test samples (C3–C75) lost compressive strength from 2% to 37% compared to the control sample.

The reduction in the compressive strength as the number of ANH increases in the total binder amount can be explained by the binding abilities of these two binders. It is known that the strength and binding ability of cement are higher than gypsum derivative binders. As the gypsum replacement level for cement increased, the compressive strength of the cube specimens decreased as expected because the cement ratio decreased. In addition, the increase in the use of gypsum together with cement also increases the pore volume [27], resulting in a loss in compressive strength.

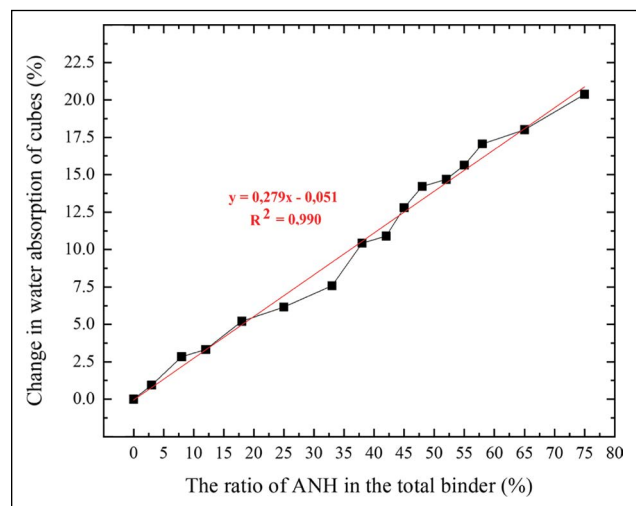
### 3.1.2. Unit Weight

Figure 5 shows the unit weight values for the fifteen trial mixtures at 28 days of curing. The unit weight value of the reference batch was  $762 \text{ kg/m}^3$  (i.e., 100%). The unit weight indices of cube specimens were linearly decreased with increasing ANH replacement levels. In cube specimens, unit weights of test specimens (C3–C75) decreased from 0.52% to 3.94% compared to the control specimen. The main reason for this decrease in unit weight is the increase in the use of gypsum derivative anhydrite III in the matrix structure.

Filling and partitioning, non-load bearing walls seem to be the top building domain of application of lightweight concrete masonry units made of LCHC. Therefore, lightness, material integrity, adequate durability, good thermal and acoustic insulation ability, cost, and sustainability are some expected material properties [36]. LCHC blocks are a non-structural element that can be used for non-load-bearing applications. However, this type of masonry unit must present a particular compressive strength [37]. It is well-known that, in general, strength increases with an increase in density. For instance, the cube specimens' unit weights and compressive strengths were compared and shown in Figure 6.



**Figure 6.** Relation between unit weight and compressive strength of cube specimens.



**Figure 7.** The effect of ANH replacement level on water absorption of cube specimens.

### 3.1.3. Water absorption

Cement-based products can be widely used in industrial applications in the external atmosphere or outdoor conditions. For this reason, the resistance of such building materials to the effect of water and their resistance to water rising as capillaries or absorbed into the material is very important. In other words, as with all material derivatives, the basic principle of cementitious materials absorbing water at the minimum level possible and impermeable to water when water affects should be sought. In this context, the capillary water permeability assessment of mortar materials is also essential. Thus, a water absorption test was performed on cube samples as the easiest and most common durability parameter. However, in light concrete derivative materials, the products are produced from highly porous

aggregates, and also the structure of the product's structure is also designed with a porous structure for the material to have light characteristics.

For this reason, it is expected that this type of product will have a very high water absorption characteristic. At this point, the importance of water absorption characteristics of lightweight concrete derivative products becomes more critical in determining mechanical and transport properties as with other building products [38]. The water absorption properties of the cube samples are shown in Figure 7.

Results indicate that as the amount of ANH increases in the total binder amount, the water absorption of the specimens increases considerably, as seen in Figure 7. When the water absorption of the reference cube specimen is assumed to be zero (0%) as a starting point, the water absorption rate of the samples increases as the ANH replacement level for cement increases. When it is evaluated with the lowest replacement level of 3% (C3), these test specimens absorbed approximately 1% by mass more water compared to the reference specimen, and when it is evaluated with the highest displacement ratio of 75% (C75), these test specimens absorbed approximately 20% more water by mass compared to the reference specimen. It has been determined that the ANH replacement level and the water absorption characteristic of the cube specimens are directly proportional. As the ANH replacement level increased, the water absorption rate of the samples increased. The possible reason is that, like other gypsum derivatives, the anhydrite III increases the cement matrix's total pore volume and causes an expansion in pore sizes. Similar results were reported by Khatib et al. [27]. In the final product, which already has high porosity due to its light structure, the different porosity of the matrix structure strengthens essential features such as heat and sound insulation.

### 3.1.4 Initial Hardening Time

LCHC blocks are cast into molds with Vibro-compacting, de-molded immediately, and transferred to a storage area for curing for up to 28 days in normal air conditions. Since LCHC blocks are removed from the mold immediately after pouring in a new concrete state, they can be deformed before they reach sufficient hardening due to casting errors or effects from the external environment. These errors can cause different products to be produced, increasing costs. By accelerating the hardening times of the products, different factors can prevent them from being quickly deformed.

Another handicap regarding the hardening times of the fully cementitious LCHC specimens is the curing time of final products for 28-day final strength. In other words, the block products' storage cost incurred during the curing period to reach their final strength. Before the block products reach the user, they are cured for 28 days for the cement to gain its real strength. This creates a storage cost.

For these two reasons, the early strength of block products is considered advantageous. Anhydrite III binder was used in this study to give early strength to the products. It is advantageous to give products early strength to increase the speed and capacity of production and reduce storage time.

In this study, the value defined as the *initial hardening time* was evaluated as the time required for the cube specimens to reach a strength value of 1 MPa from when they were removed from the mold. The value of 1 MPa has been experienced as the appropriate strength value predicted in real applications regarding the transport of the specimens to the area to be applied, the required strength, and permanence during the application. For this reason, it has been accepted, based on the author's experience, that the blocks produced from specimens reaching a compressive strength of 1 MPa are suitable for real applications. The examination of the time taken for the cube specimens to reach a compressive strength value of 1 MPa after being removed from the mold is represented in Figure 8.

When Figure 8 is examined, the initial hardening time of the control batch is 443 min. For cube specimens with ANH replacement levels up to 45% for cement, the initial hardening time rapidly decreased to 89%. Although there is a reduction in initial hardening time after 45% replacement (C45), this reduction has a slowing trend. The initial hardening time of the B15 specimen with the highest replacement level of 75% (C75) is 94.6% quicker than the control specimen. This increase in the setting time is associated with the fact that anhydrite III reacts very quickly with the mixing water and provides a very fast hardening of the total binder. The setting starts when the anhydrite III in the test mixture reacts quickly with water and turns into calcium sulfate dihydrate. Kovler [39] studied the triple mixture of gypsum, cement, and silica fume. Similarly, the researcher determined that the setting of this triple mixture started in 5 minutes with the conversion of calcium sulfate hemihydrate into calcium sulfate dihydrate. This experimental study determined that early strength was gained rapidly when ANH was added to the mixtures.

## 3.2. LCHC Block Specimens

In the second stage of the study, LCHC block specimens were produced, and these specimens' physical and mechanical properties were determined. The physical and mechanical properties of the LCHC block specimens are summarized in Table 5.

The mixtures were coded according to the ANH material addition, where "B" defines the LCHC block specimens, "M1, M2, M3" defines the model of LCHC block, and the numbers 0 to 75 define the replacement level of ANH by cement by weight.

### 3.2.1. Block Mass

The block mass of a lightweight concrete masonry block is expressed as the oven-dry mass of the block in kg. In production, the density of a given concrete masonry unit is

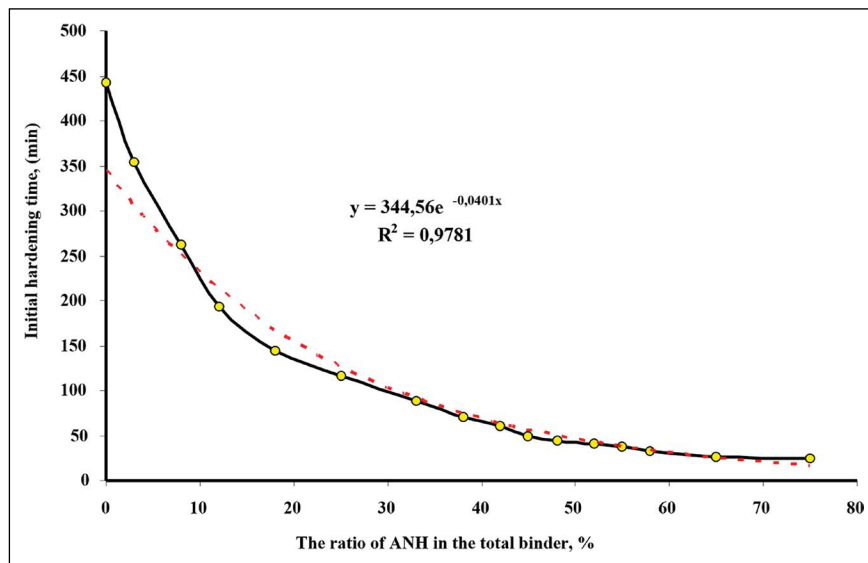


**Figure 8.** Effect of ANH replacement on initial hardening time of cube specimens.

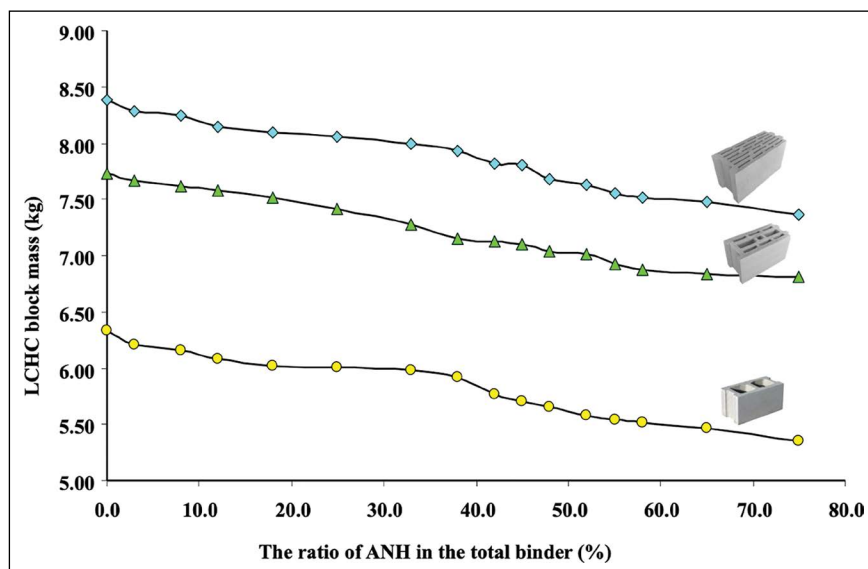


**Figure 9.** Effect of ANH replacement level on the mass of LCHC block specimens.

partly controlled by the methods used to manufacture the unit but mainly by the type of aggregate used in production [40]. Through the use of lightweight aggregates, the resulting density of lightweight concrete masonry units can be varied by the producer to achieve one or more desired physical properties. Block dry density or dry mass, however, can influence other structural design considerations aside from compressive strength. Reducing the density of a concrete masonry unit can reduce the overall weight of a structure and potentially reduce the required size of the supporting foundation and the structural members. Reducing the mass of a structure or element also reduces the seismic load a structure or element must be designed to resist because the magnitude of seismic loading is a direct function of dead

load [40]. In this context, the oven-dry masses of the blocks were measured, and the results are represented in Figure 9.

The mass of LCHC blocks decreases as the percentage of ANH replacement increases. This is due to the lower specific gravity of ANH (2.30) compared to fine aggregate (3.15). Also, entrapped air caused by the use of anhydrite III may contribute to the reduction in mass of the LCHC blocks. Masses of the hollow blocks varied between 5.35 kg and 6.33 kg for M1, 6.81 kg and 7.73 kg for M2, and 7.36 kg and 8.38 kg for M3. In general, the experience for this reduction for the hollow blocks used in this research was approximately 1% block mass reduction versus a 5.70% increase in ANH replacement level for cement. Assuming the mass of normal-weight aggregate concrete masonry for

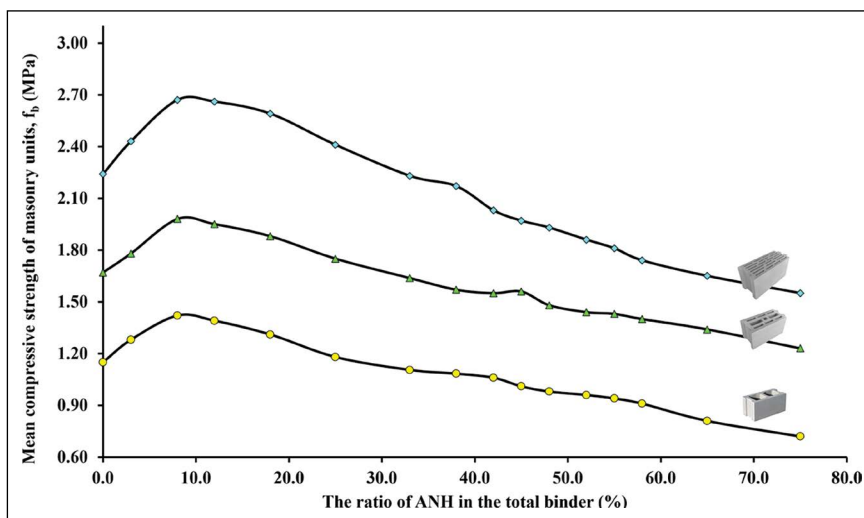


Figure 10. Effect of ANH replacement level on compressive strength of LCHC blocks.

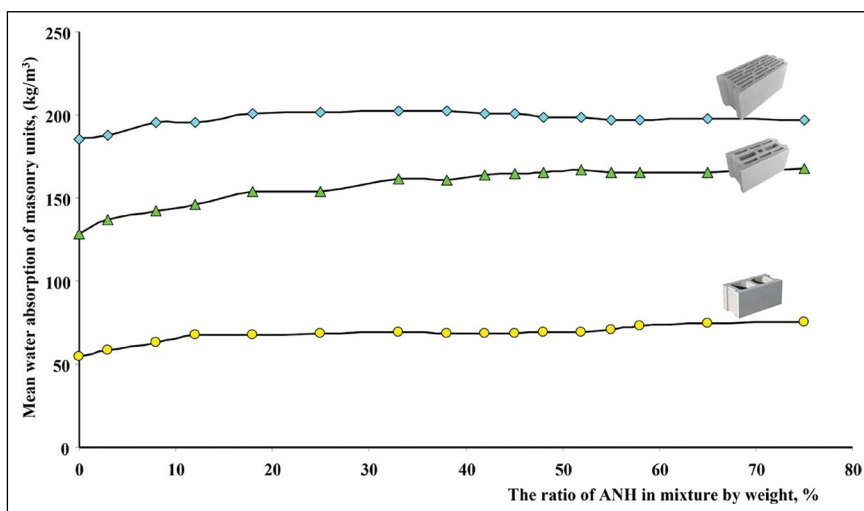


Figure 11. Effect of ANH replacement level on water absorption of LCHC blocks.

non-load bearing walls and partitions vary between 14 kg and 27 kg depending on their unit design geometry, the research showed that LCHC blocks are 61% to 80% lighter than normal-weight concrete masonry units.

### 3.2.2. Compressive Strength

The compressive strengths of the LCHC blocks, made from cement, ANH, and lightweight aggregates containing 16 mixtures, are shown in Figure 10.

It can be seen from Figure 10 that non-load-bearing LCHC blocks can be produced by using ANH replacement for cement. Generally, it can be noticed that the compressive strength of LCHC decreased as the percentage of ANH replacement level increased. The strength reduction is due to the weaker bonding ability of gypsum-based binders compared to Portland cement. Furthermore, the air-entraining property (when used with cement) of ANH binder reduces the bonding area within the concrete matrix. This phenom-

enon also causes a reduction in compressive strength. However, compressive strength reduction starts with an 8% ANH replacement level (B8). Above the 8% ANH replacement level, the compressive strengths of the LCHC block decreased continuously. On the contrary, utilization of 3% (C3) and 8% (C8) ANH replacement levels resulted in an increase in compressive strength as 11.30% and 23.5% for M1, 6.60% and 18.50% for M2, and 8.50% and 19.20% for M3, respectively.

There has been observed to be an increase in cement replacement rates up to 8% of the ANH ratio in mixtures in block production, which can be considered linear in block compressive strength values. It has been experienced that this increase in the strength value causes the mineral formations in the matrix structure that form strength earlier to develop more rapidly due to the anhydride ratio and the amount of cement contained in the mixture composition, and the edge and angular units in the geometric form of the block to form in a more compact structure, which has

a strength-enhancing effect. Furthermore, up to a 25% replacement level, all test specimens' compressive strength values were higher than the compressive strength value of the reference block specimen. However, it has been experienced that minerals formed as a result of hydration at anhydride utilization rates higher than 8% cause the matrix structure to acquire a more brittle form, which leads to a decrease in strength values.

### 3.2.3. Water Absorption

Lightweight hollow concrete masonry unit specifications typically establish upper limits on the amount of water permitted to be absorbed. Expressed in a kilogram of water per cubic meter of concrete, these limits vary with the density classification of the unit. Although no limit value for water absorption has been stated in BS 6073: Part 1 for the concrete masonry units, US National Concrete Masonry Association proposes that the maximum water absorption should be lower than 288 kg/m<sup>3</sup> for lightweight concrete masonry units [40]. The mean values for water absorption of LCHC blocks are given in Table 6. This table clearly shows that all absorption values are 54.4 kg/m<sup>3</sup> and 201.7 kg/m<sup>3</sup>, within the acceptable water absorption values according to the US National Concrete Masonry Association recommendation. The research findings are represented in Figure 11.

While the absorption values are not directly related to masonry units' physical and geometrical properties such as dimension, pore size, and mechanisms of deterioration such as freeze-thaw, they provide a measure of the void structure within the lightweight concrete of the masonry unit. Several production variables can affect the void structure, including the plastic mix's degree of compaction, binder and water content, aggregate gradation, and the parameters of the mixing operation. Due to the vesicular structure of lower-density units, there is a potential for higher measured absorption than is typical for higher-density units [40]. This effect is observed in LCHC blocks almost for all mixes. Besides, the ANH replacement level increase appeared as a slight increase in the water absorption characteristics in all three block designs. LCHC blocks, already porous products by nature, are expected to have higher water absorption properties. Furthermore, the amount of water absorption increased more with the enlargement of the pore sizes in the cement matrix by adding ANH.

Table 6. Physical characteristics of the LCHC block specimens

Mix	A/B	Block mass (kg)			Compressive strength (N/mm <sup>2</sup> )			Water absorption (kg/m <sup>3</sup> )			Thermal Conductivity (W/mK)		
		M1	M2	M3	M1	M2	M3	M1	M2	M3	M1	M2	M3
B0	3.73	6.33	7.73	8.38	1.15	1.67	2.24	54.4	128.1	185.1	0.267	0.196	0.155
B3	3.75	6.21	7.66	8.28	1.28	1.78	2.43	58.3	137.1	187.6	0.263	0.195	0.157
B8	3.77	6.16	7.62	8.25	1.42	1.98	2.67	62.7	142.3	195.7	0.263	0.194	0.157
B12	3.80	6.08	7.58	8.15	1.39	1.95	2.66	67.4	146.4	195.1	0.255	0.194	0.155
B18	3.83	6.02	7.52	8.10	1.31	1.88	2.59	67.5	154.1	200.5	0.252	0.193	0.154
B25	3.87	6.01	7.41	8.06	1.18	1.75	2.41	68.2	153.5	201.7	0.251	0.191	0.154
B33	3.92	5.98	7.28	8.00	1.11	1.64	2.23	68.9	161.8	202.6	0.250	0.188	0.153
B38	3.95	5.92	7.15	7.93	1.08	1.57	2.17	68.7	160.5	202.3	0.246	0.186	0.152
B42	3.98	5.77	7.13	7.82	1.06	1.55	2.03	68.4	164.1	200.6	0.238	0.185	0.150
B45	4.00	5.71	7.10	7.80	1.01	1.56	1.97	68.5	164.9	201.0	0.235	0.185	0.150
B48	4.01	5.65	7.04	7.68	0.98	1.48	1.93	69.4	165.5	198.7	0.232	0.184	0.148
B52	4.04	5.58	7.01	7.63	0.96	1.44	1.86	69.4	166.8	198.5	0.228	0.183	0.148
B55	4.06	5.54	6.92	7.55	0.94	1.43	1.81	70.8	165.1	197.2	0.225	0.181	0.146
B58	4.08	5.51	6.87	7.51	0.91	1.40	1.74	72.8	165.4	196.9	0.224	0.180	0.146
B65	4.13	5.46	6.84	7.48	0.81	1.34	1.65	74.5	165.7	198.0	0.221	0.180	0.145
B75	4.20	5.35	6.81	7.36	0.72	1.23	1.55	75.2	167.4	197.3	0.215	0.179	0.143

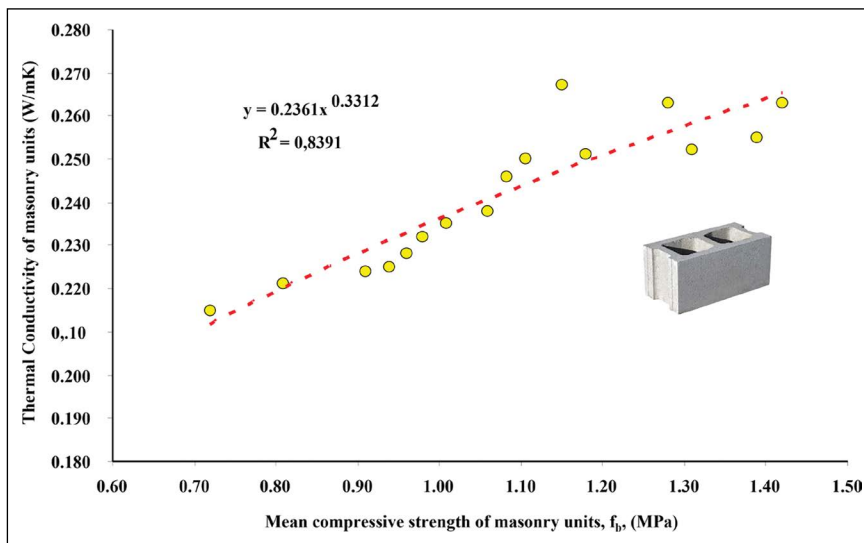


Figure 12. Compressive strength versus thermal conductivity values of LCHC model 1 blocks.

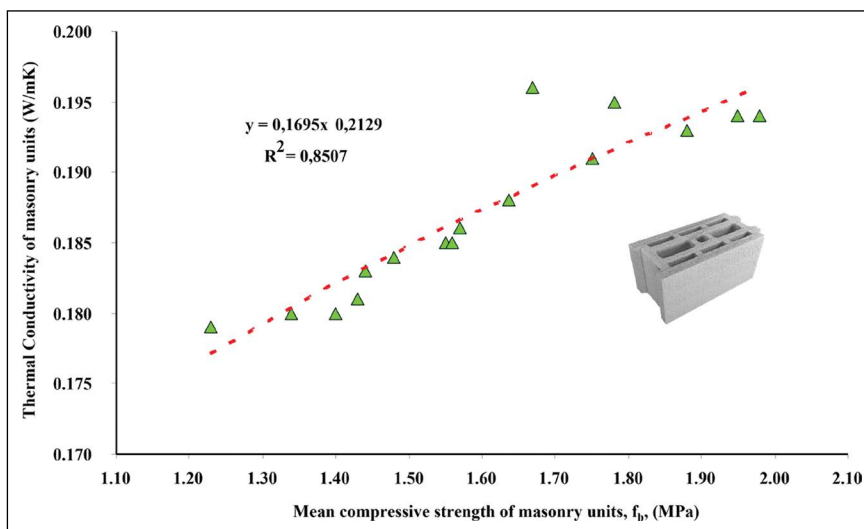


Figure 13. Compressive strength versus thermal conductivity values of LCHC model 2 blocks.

### 3.2.4. Thermal Conductivity

The thermal properties of the masonry blocks analyzed are given in Table 6 for three different LCHC block models. Each block type can be produced from lightweight concrete of different densities and black masses. The different mass values directly influence the thermal properties of lightweight concrete masonry blocks. It can be easily noticed from Table 6 that the thermal conductivity coefficients of the blocks decrease depending on the decrease in the mass of the blocks. The thermal conductivity values of model 1 blocks vary between 0.215 W/mK and 0.267 W/mK, the thermal conductivity values of model 2 blocks vary between 0.179 W/mK and 0.196 W/mK, and the thermal conductivity values of model 3 blocks vary between 0.143 W/mK and 0.155 W/mK. For all three types of block products, it was determined that as the ANH replacement level

for cement increased, the thermal conductivity values of the block products decreased. From this, it is concluded that using cement and anhydrite III binder together harms the overall compressive strength but significantly improves the thermal insulation performance of the block products. In order to both compare the thermal performances and compressive strengths of all three models of block samples and to approximately determine the thermal conductivity ( $\lambda$ ) value of a block product whose compressive strength is determined; in Figure 12, Figure 13, and Figure 14, the compressive strength values versus the thermal conductivity values of the model 1, model 2 and model 3 block specimens, respectively, are represented.

According to Figures 12–14, as the compressive strength values of all three model block samples decrease, the thermal conductivity values also decrease. In other

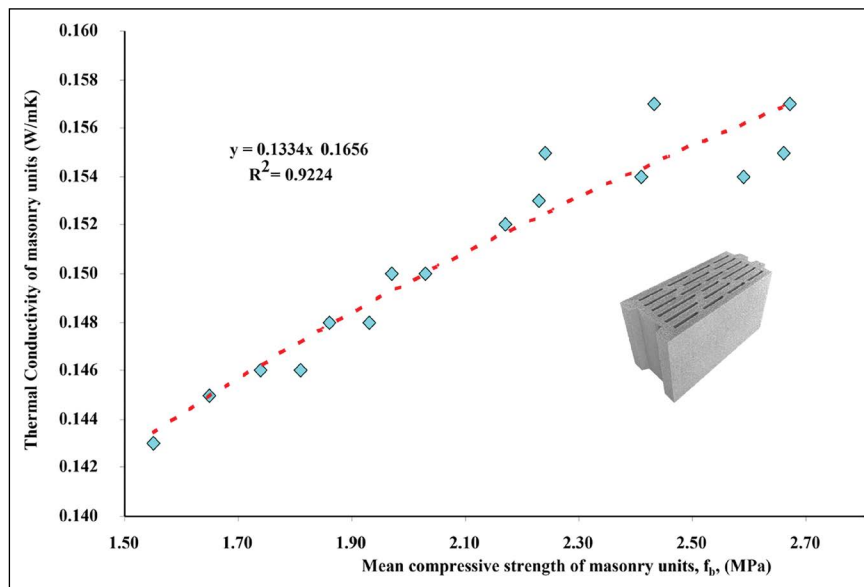


**Figure 14.** Compressive strength versus thermal conductivity values of LCHC model 3 blocks.

words, as the ANH displacement rate increases, the unit weights of the specimens decrease, and accordingly, the compressive strength values and thermal conductivity values decrease. Thus, their performance in terms of thermal insulation is improved. It has been determined that model 3 block specimens perform better than the other two model block samples in terms of compressive strength and thermal conductivity.

The compressive strength of the blocks can be determined in a shorter time and more efficiently than the determination of the thermal conductivity coefficient. In addition, a relationship was determined between the compressive strength and thermal conductivity values of the block samples produced for all three models tested within the scope of the study. Therefore, a formula has been proposed by which the thermal conductivity coefficient of the blocks can be determined by using the compressive strength of the blocks, which is determined relatively quickly, and the net fullness ratio, covering all three block models (Eq. 1).

$$\lambda_b = \frac{1.101}{e^{0.191 \times \eta}} \times f_b^{\left(\frac{2.212}{e^{0.237 \times \eta}}\right)} \quad (1)$$

Where  $\lambda_b$  is the thermal conductivity coefficient of a single block,  $f_b$  is the compressive strength of a single block, and  $\eta$  is the net fullness ratio of the single block.

### 3.3. Wall Section Model

The scope of the masonry tests on the wall section model is to determine the wall's characteristic compressive strength ( $f_k$ ) and modulus of elasticity ( $E_k$ ). The wall model is represented in Figure 3. In this wall section, there was no mortar in the vertical direction between the LCHC blocks, but 0.7 mm masonry mortar was applied in the horizontal direction between the LCHC blocks.

Eurocode 6 [41] gives a relation between the mean compressive strength of a masonry unit and the characteristic compressive strength of masonry ( $f_k$ ):  $f_k = 0.5 \times f_b^{0.85}$ . The results obtained from this study and the Eurocode 6 estimation is represented in Figure 15.

According to Eurocode 6 [41], the thickness of bed joints of 0.5 mm to 3 mm ensures that the thin layer mortar has been applied, and thin layer mortar applications are not taken into account when calculating the compressive strength of the wall. In Figure 15, the results of the masonry model's characteristic compressive strength ( $f_k$ ) and the normalized mean compressive strength of the masonry units ( $f_b$ ) are shown, and the comparison of Eurocode 6 and the results of this work is given.

Test results show that the characteristic compressive strength of the tested thin joint hollow concrete masonry with lightweight aggregates could be estimated by the equation given by Eurocode 6. When the compressive strength of the wall model obtained with LCHC blocks with relatively low compressive strengths is calculated, the results are more suitable for Eurocode 6, but as the compressive strength of the block increases, higher wall compressive strengths ( $f_k$ ) are obtained than the formula values defined by Eurocode 6. Thus, an alternative formulation is proposed that includes the results of all three models in order to make a more precise inference (Eq. 2):

$$f_k = 0.526 \times f_b^{0.985} \quad (2)$$

In Figure 16, the elasticity modulus of the masonry section is given.

When Figure 16 is examined, as expected, the elastic modulus of the wall section increases as the compressive strength of the LCHC blocks forming the wall section increases. Using the results of the compressive strengths of three different models of LCHC blocks, the modulus of elasticity formula of the wall section was determined (Eq. 3).

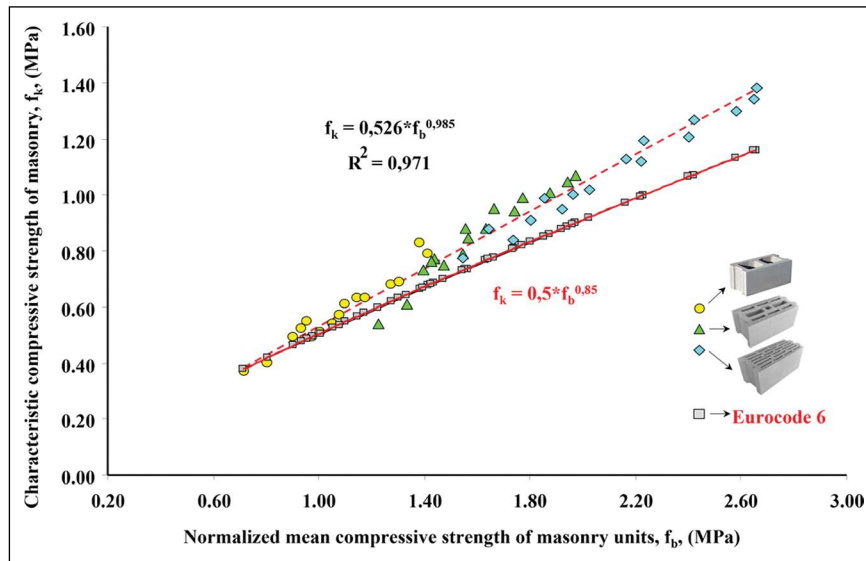


Figure 15. Characteristic compressive strength of the masonry section and comparison with Eurocode 6.

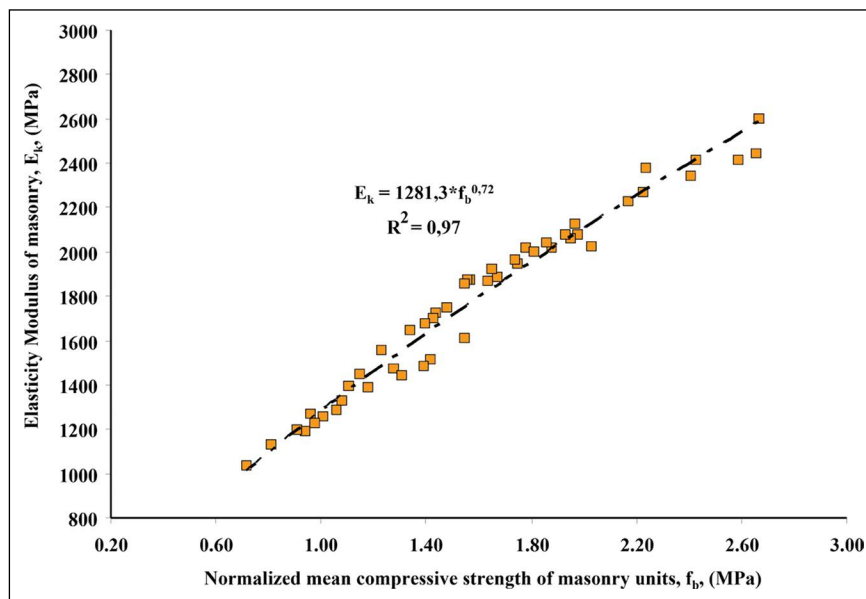


Figure 16. The elasticity modulus of the masonry section.

$$E_k = 1281.3 \times f_b^{0.72} \quad (3)$$

#### 4. CONCLUSIONS

The properties of lightweight hollow concrete masonry units made of CEM I, anhydrite III, expanded perlite, pumice, and calcite were investigated in this research work. In particular, the changes in the physical and mechanical properties of lightweight concrete and lightweight masonry block products resulting from replacing anhydrite III with cement in specific proportions were investigated. It was possible to manufacture standard shape and size LCHC blocks using dry, too-stiff consistency mixtures to keep their shape

and size during the demolding, curing, and hardening processes. The dry densities of the LCHC blocks complied with the standard acceptable limits for lightweight hollow concrete masonry units (i.e., less than 880 kg/m<sup>3</sup>).

The research findings show that the higher the ANH replacement level for cement in the mixture, the lesser the dry density and block mass of LCHC blocks. In cube specimens, unit weights of test specimens decreased from 0.52% to 3.94% compared to the control specimen, when the ANH replacement level started from 3% to 75% for cement, respectively. Similarly, the increase in the ANH displacement ratio in masonry block products caused a decrease in the weight of the block products.

In cube specimens, test specimens (C3–C75) lost compressive strength from 2% to 37% compared to the control specimen. However, it has been observed that there is an increase in compressive strength values of LCHC block products with ANH replacement levels of up to 8% in mixtures. Furthermore, up to a 25% replacement level, all test specimens' compressive strength values were higher than the compressive strength value of the reference block specimen. However, the 8% ANH replacement ratio was determined as the optimum value.

When it is evaluated with the lowest replacement level of 3% (C3), these cubic test specimens absorbed approximately 1% by mass more water compared to the reference specimen, and when it is evaluated with the highest displacement ratio of 75% (C75), these cubic test specimens absorbed approximately 20% more water by mass compared to the reference specimen. Similarly, the ANH replacement level increase appeared as a slight increase in the water absorption characteristics in all three block designs (M1, M2, M3).

For cube specimens with ANH replacement levels up to 45% for cement, the initial hardening time rapidly decreased to 89%. Although there is a reduction in initial hardening time after 45% replacement (C45), this reduction has a slowing trend. The initial hardening time of the B15 specimen with the highest replacement level of 75% (C75) is 94.6% quicker than the control specimen.

The thermal conductivity values of Model 1 blocks vary between 0.215 W/mK and 0.267 W/mK, the thermal conductivity values of Model 2 blocks vary between 0.179 W/mK and 0.196 W/mK, and the thermal conductivity values of Model 3 blocks vary between 0.143 W/mK and 0.155 W/mK. For all types of block products, it was determined that as the ANH replacement level for cement increased, the thermal conductivity values of the block products decreased. Furthermore, a formula has been proposed by which the thermal conductivity coefficient of the blocks can be determined by using the compressive strength of the blocks and the net fullness ratio, which are determined relatively easily, covering all three block models (Eq. 1).

When the compressive strength of the wall model obtained with LCHC blocks with relatively low compressive strengths is calculated, the results are more suitable for Eurocode 6, but as the compressive strength of the block increases, higher wall compressive strengths ( $f_k$ ) are obtained than the formula values defined by Eurocode 6. Thus, an alternative formulation is proposed that includes the results of all three models in order to make a more precise inference (Eq. 2). Also, by using the results of the compressive strengths of three different models of LCHC blocks, the modulus of elasticity formula of the wall section was determined (Eq. 3).

## ETHICS

There are no ethical issues with the publication of this manuscript.

## DATA AVAILABILITY STATEMENT

The authors confirm that the data that supports the findings of this study are available within the article. Raw data that support the finding of this study are available from the corresponding author, upon reasonable request.

## CONFLICT OF INTEREST

The authors declare that they have no conflict of interest.

## FINANCIAL DISCLOSURE

The authors declared that this study has received no financial support.

## PEER-REVIEW

Externally peer-reviewed.

## REFERENCES

- [1] Gündüz, L., & Kalkan, Ş. O. (2020). Lightweight cellular hollow concrete blocks containing volcanic tuff powder, expanded clay, and diatomite for non-load bearing walls. *Teknik Dergi*, 31(6), 10291–10313. [\[CrossRef\]](#)
- [2] Gündüz, L. (2008). Use of quartet blends containing fly ash, scoria, perlite pumice and cement to produce cellular hollow lightweight masonry blocks for non-load bearing walls. *Construction and Building Materials*, 22(5), 747–754. [\[CrossRef\]](#)
- [3] Türkmenoğlu, A. G., & Tankut, A. (2002). Use of tuffs from central Turkey as admixture in pozzolanic cements: Assessment of their petrographical properties. *Cement and Concrete Research*, 32(4), 629–637. [\[CrossRef\]](#)
- [4] Faella, G., Manfredi, G., & Realfonzo, R. (1992). Cyclic behaviour of tuff masonry walls under horizontal loadings. In *Proc. 6<sup>th</sup> Can. Masonry Symp.*, Canada, 317–328.
- [5] ASTM. (2005). *Annual book of ASTM standards, book of standards section 4 – construction, Volume 04.02 and 04.03*. ASTM International.
- [6] Gündüz, L. (2005). A technical report on lightweight aggregate masonry block manufacturing in Turkey. *Suleyman Demirel University*, 1, 110.
- [7] Şapcı, N., Gündüz, L., & Yağmurlu, F. (2014). Usage of Aksaray ignimbrites as natural lightweight aggregate and evaluation of the production for lightweight hollow masonry units. *Pamukkale University Journal of Engineering Sciences*, 20(3), 63–69. [\[CrossRef\]](#)
- [8] Al-Tamimi, A. S., Al-Amoudi, O. S. B., Al-Osta, M. A., Ali, M. R., & Ahmad, A. (2020). Effect of insulation materials and cavity layout on heat transfer of concrete masonry hollow blocks. *Construction and Building Materials*, 254, Article 119300. [\[CrossRef\]](#)

- [9] Al-Hadhrami, L. M., & Ahmad, A. (2009). Assessment of thermal performance of different types of masonry bricks used in Saudi Arabia. *Applied Thermal Engineering*, 29(5-6), 1123–1130. [CrossRef]
- [10] Sengul, O., Azizi, S., Karaosmanoglu, F., & Tasdemir, M. A. (2011). Effect of expanded perlite on the mechanical properties and thermal conductivity of lightweight concrete. *Energy and Buildings*, 43(2-3), 671–676. [CrossRef]
- [11] The Portland Cement Association. (2016). (Dec 09, 2022). *Concrete masonry units*. <https://www.cement.org/cement-concrete/products/concrete-masonry-units>
- [12] Lushnikova, N., & Dvorkin, L. (2016). Sustainability of gypsum products as a construction material. In *Sustainability of Construction Materials* (pp. 643–681). Woodhead Publishing. [CrossRef]
- [13] Powell, D. A. (1958). Transformation of the  $\alpha$ - and  $\beta$ -forms of calcium sulphate hemihydrate to insoluble anhydrite. *Nature*, 182(4638), Article 792. [CrossRef]
- [14] Bensted, J., & Prakash, S. (1968). Investigation of the calcium sulphate-water system by infrared spectroscopy. *Nature*, 219(5149), 60–61. [CrossRef]
- [15] Odler, I. (2000). *Special inorganic cements*. Taylor & Francis.
- [16] Macia, E., Dubois, J-M., & Thiel, P. A. (1985). *Ullmann's encyclopedia of industrial chemistry*. Wiley.
- [17] Sievert, T., Wolter, A., & Singh, N. B. (2005). Hydration of anhydrite of gypsum ( $\text{CaSO}_4 \cdot \text{II}$ ) in a ball mill. *Cement and Concrete Research*, 35(4), 623–630. [CrossRef]
- [18] Binici, H., Kapur, S., Arocena, J., & Kaplan, H. (2012). The sulphate resistance of cements containing red brick dust and ground basaltic pumice with sub-microscopic evidence of intra-pore gypsum and ettringite as strengtheners. *Cement and Concrete Composites*, 34(2), 279–287. [CrossRef]
- [19] Hossain, K. M. A. (2003). Blended cement using volcanic ash and pumice. *Cement and Concrete Research*, 33(10), 1601–1605. [CrossRef]
- [20] Kabay, N., Tufekci, M. M., Kizilkanat, A. B., & Oktay, D. (2015). Properties of concrete with pumice powder and fly ash as cement replacement materials. *Construction and Building Materials*, 85, 1–8. [CrossRef]
- [21] Torkaman, J., Ashori, A., & Momtazi, A. S. (2014). Using wood fiber waste, rice husk ash, and limestone powder waste as cement replacement materials for lightweight concrete blocks. *Construction and Building Materials*, 50, 432–436. [CrossRef]
- [22] Duan, P., Shui, Z., Chen, W., & Shen, C. (2013). Enhancing microstructure and durability of concrete from ground granulated blast furnace slag and metakaolin as cement replacement materials. *Journal of Materials Research and Technology*, 2(1), 52–59. [CrossRef]
- [23] Mehta, P. K., & Monteiro, P. J. (2014). *Concrete: Microstructure, properties, and materials*. McGraw-Hill Education.
- [24] Naik, T. R., Kumar, R., Chun, Y. M., & Kraus, R. N. (2010). *Utilization of Powdered gypsum-wallboard in concrete*. In *Proceedings International Conference Sustainable Constructions Materials Technologies*.
- [25] Escalante-Garcia, J. I., Martínez-Aguilar, O. A., & Gomez-Zamorano, L. Y. (2017). Calcium sulphate anhydrite based composite binders; effect of Portland cement and four pozzolans on the hydration and strength. *Cement and Concrete Composites*, 82, 227–233. [CrossRef]
- [26] Hansen, S., & Sadeghian, P. (2020). Recycled gypsum powder from waste drywalls combined with fly ash for partial cement replacement in concrete. *Journal of Cleaner Production*, 274, Article 122785. [CrossRef]
- [27] Khatib, J. M., Wright, L., & Mangat, P. S. (2013). Effect of fly ash-gypsum blend on porosity and pore size distribution of cement pastes. *Advances in Applied Ceramics*, 112(4), 197–201. [CrossRef]
- [28] British Standards Institution. (1995). *BS 812: Part 2, Testing aggregates. Methods for determination of density*. British Standards Institution.
- [29] British Standards Institution. (1990). *BS 812: Part 110, Testing aggregates. Methods for determination of aggregate crushing value (ACV)*. British Standards Institution.
- [30] ASTM. (2004). *ASTM C127-04, Standard test method for density, relative density (specific gravity), and absorption of coarse aggregate*. ASTM International.
- [31] ASTM. (2004) *ASTM C128-04, Standard test method for density, relative density (specific gravity), and absorption of fine aggregate*. ASTM International, West Conshohocken, PA," 2004.
- [32] Turkish Standards Institution. (2015). *TS EN 771-3+A1, Specification for masonry units - Part 3: Aggregate concrete masonry units (Dense and lightweight aggregates)*. Turkish Standards Institution.
- [33] British Standards Institution. (1986). *BS 1881: Part 125, Testing concrete. Methods for mixing and sampling fresh concrete in the laboratory*. British Standards Institution.
- [34] British Standards Institution. (1983). *BS 1881: Part 114, Testing concrete. Methods for determination of density of hardened concrete*. British Standards Institution.
- [35] British Standards Institution. (1981). *BS 6073: Part 1, Precast concrete masonry units. Specification for precast concrete masonry units*. British Standards Institution.
- [36] Faustino, J., Silva, E., Pinto, J., Soares, E., Cunha, V. M., & Soares, S. (2015). Lightweight concrete masonry units based on processed granulate of

- corn cob as aggregate. *Materiales de Construcción*, 65(318), Article e055. [CrossRef]
- [37] British Standards Institution. (2011). (Dec 09, 2022). *BS EN 771-3, Specification for masonry units. Aggregate concrete masonry units (dense and lightweight aggregates)*. British Standards Institution. [https://www.en-standard.eu/bs-en-771-3-2011-a1-2015-specification-for-masonry-units-aggregate-concrete-masonry-units-dense-and-lightweight-aggregates/?gclid=Cj0KCQiA1sucBhDgARIsAFoytUtgPd8N-5WkaafFDB\\_VaHfY0o90I4baU43G9DQ-I862y2Sv-J0296GRgaAra9EALw\\_wcB](https://www.en-standard.eu/bs-en-771-3-2011-a1-2015-specification-for-masonry-units-aggregate-concrete-masonry-units-dense-and-lightweight-aggregates/?gclid=Cj0KCQiA1sucBhDgARIsAFoytUtgPd8N-5WkaafFDB_VaHfY0o90I4baU43G9DQ-I862y2Sv-J0296GRgaAra9EALw_wcB) Accessed on Dec 16, 2022.
- [38] Yan, S., Sagoe-Crentsil, K., & Shapiro, G. (2012). Properties of cement mortar incorporating de-inking waste-water from waste paper recycling. *Construction and Building Materials*, 29, 51–55. [CrossRef]
- [39] Kovler, K. (1998). Setting and hardening of gypsum-portland cement-silica fume blends, Part 1: temperature and setting expansion. *Cement and Concrete Research*, 28(3), 423–437. [CrossRef]
- [40] Masonry Advisory Council, (2007). Density-related properties of concrete masonry. *Building Construction & Design Viewpoint*, 1(1), 1–4.
- [41] Turkish Standards Institution. (2013). (Dec 09, 2022). *TS EN 1996-1-1:2005+A1, Eurocode 6 - Design of masonry structures - Part 1-1: General rules for reinforced and unreinforced masonry structures*. Turkish Standart Institutions. [https://www.en-standard.eu/bs-en-1996-1-1-2005-a1-2012-eurocode-6-design-of-masonry-structures-general-rules-for-reinforced-and-unreinforced-masonry-structures/?gclid=Cj0KCQiA1sucBhDgARIsAFoytUs\\_2bX5SS1dUwRNNbQfhG7cuoT5cVhZW-IxC4B8omVbaOcUVlL12b4aAuPhEALw\\_wcB](https://www.en-standard.eu/bs-en-1996-1-1-2005-a1-2012-eurocode-6-design-of-masonry-structures-general-rules-for-reinforced-and-unreinforced-masonry-structures/?gclid=Cj0KCQiA1sucBhDgARIsAFoytUs_2bX5SS1dUwRNNbQfhG7cuoT5cVhZW-IxC4B8omVbaOcUVlL12b4aAuPhEALw_wcB) Accessed on Dec 16, 2022.